

# Heterogeneity-Informed Meta-Parameter Learning for Spatiotemporal Time Series Forecasting

Zheng Dong\*  
Southern University of  
Science and Technology  
zhengdong00@outlook.com

Renhe Jiang\*  
The University of Tokyo  
jiangrh@csis.u-tokyo.ac.jp

Haotian Gao  
The University of Tokyo  
gaoht6@outlook.com

Hangchen Liu  
Southern University of  
Science and Technology  
liuhc3@outlook.com

Jinliang Deng  
Hong Kong University of  
Science and Technology  
dengjinliang@ust.hk

Qingsong Wen  
Squirrel AI  
qingsongedu@gmail.com

Xuan Song<sup>†</sup>  
Jilin University  
Southern University of  
Science and Technology  
songx@sustech.edu.cn

## ABSTRACT

Spatiotemporal time series forecasting plays a key role in a wide range of real-world applications. While significant progress has been made in this area, fully capturing and leveraging spatiotemporal heterogeneity remains a fundamental challenge. Therefore, we propose a novel **Heterogeneity-Informed Meta-Parameter Learning** scheme. Specifically, our approach implicitly captures spatiotemporal heterogeneity through learning spatial and temporal embeddings, which can be viewed as a clustering process. Then, a novel spatiotemporal meta-parameter learning paradigm is proposed to learn spatiotemporal-specific parameters from meta-parameter pools, which is informed by the captured heterogeneity. Based on these ideas, we develop a **Heterogeneity-Informed Spatiotemporal Meta-Network (HimNet)** for spatiotemporal time series forecasting. Extensive experiments on five widely-used benchmarks demonstrate our method achieves state-of-the-art performance while exhibiting superior interpretability. Our code is available at <https://github.com/XDZhelheim/HimNet>.

## CCS CONCEPTS

• Information systems → Spatial-temporal systems; • Computing methodologies → Artificial intelligence.

## KEYWORDS

spatiotemporal time series, heterogeneity, meta-parameter learning

## ACM Reference Format:

Zheng Dong, Renhe Jiang, Haotian Gao, Hangchen Liu, Jinliang Deng, Qingsong Wen, and Xuan Song. 2024. Heterogeneity-Informed Meta-Parameter Learning for Spatiotemporal Time Series Forecasting. In *Proceedings of the*

\*Equal contribution.

<sup>†</sup>Corresponding author.

Permission to make digital or hard copies of all or part of this work for personal or classroom use is granted without fee provided that copies are not made or distributed for profit or commercial advantage and that copies bear this notice and the full citation on the first page. Copyrights for components of this work owned by others than the author(s) must be honored. Abstracting with credit is permitted. To copy otherwise, or republish, to post on servers or to redistribute to lists, requires prior specific permission and/or a fee. Request permissions from [permissions@acm.org](mailto:permissions@acm.org).

KDD '24, August 25–29, 2024, Barcelona, Spain

© 2024 Copyright held by the owner/author(s). Publication rights licensed to ACM.  
ACM ISBN 978-1-4503-XXXX-X/24/08  
<https://doi.org/XXXXXXX.XXXXXXX>

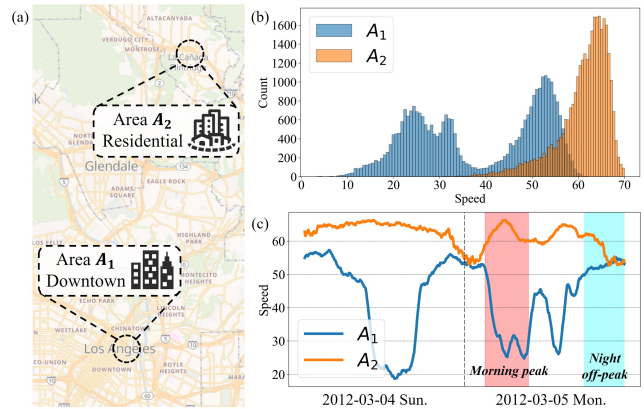


**Figure 1: Spatiotemporal heterogeneity.** (a): Locations of two selected areas.  $A_1$  is in the downtown region, while  $A_2$  is a residential area. (b): Illustration of spatial heterogeneity, with differing vehicle speed distributions between  $A_1$  and  $A_2$ . (c): Demonstration of temporal heterogeneity, showing distinct patterns between different time periods.

30th ACM SIGKDD Conference on Knowledge Discovery and Data Mining (KDD '24). ACM, New York, NY, USA, 11 pages. <https://doi.org/XXXXXXX.XXXXXXX>

## 1 INTRODUCTION

The rise of sensor networks has brought the widespread collection of spatiotemporal time series in urban environments. As these datasets grow quickly, accurate spatiotemporal time series forecasting is increasingly important for many real-world applications such as transportation [30, 32], weather [1], and economics [33]. While considerable efforts [16, 17, 20, 22, 51] have been made, existing methods still face a major challenge: fully capturing and leveraging *spatiotemporal heterogeneity*. Spatial heterogeneity refers to the phenomenon that distinct patterns are observed across different location types during the same time period, while temporal heterogeneity is reflected by the unique patterns observed at the same location across different time periods. Figure 1 provides a real-world example. As shown in Figure 1(a), we analyze two areas in

different spatial contexts: Area  $A_1$  in downtown LA and Area  $A_2$  in a residential region. Figure 1(b) reveals substantial differences in vehicle speed distributions between them:  $A_1$  shows a lower average speed due to daily downtown congestion, while  $A_2$  exhibits higher speeds with less commuting pressure. This demonstrates spatial heterogeneity. Figure 1(c) illustrates their time series in different temporal contexts. The patterns are stable during the holiday (Sun.) but fluctuate violently during the workday (Mon.). Furthermore, morning peak hours and nighttime off-peak hours also exhibit opposing trends, showing temporal heterogeneity. These phenomena occur consistently throughout spatiotemporal data. Thus, effectively modeling spatiotemporal heterogeneity is critical to accurate forecasting. As time series from diverse spatial locations and time periods display distinct characteristics, proper capturing of heterogeneity relies on identifying and distinguishing such varied spatiotemporal contexts.

To account for different contexts, graph-based approaches [36, 53, 63] attempt to capture heterogeneity by utilizing handcrafted features such as graph topology and similarity metrics between time series. However, depending heavily on **pre-defined representations** limits their adaptability and generalizability, as these features cannot encompass the full complexity of diverse contexts. To enhance adaptability, other works introduce meta-learning techniques [47, 48] that apply multiple parameter sets across different spatial locations. However, they also rely on **auxiliary characteristics** including Points-of-Interests (POIs) and sensor placements. Additionally, the **high computational and memory costs** limit their applicability to large-scale datasets. Recent representation learning methods [39, 52] effectively identify heterogeneity through input embeddings. However, their oversimplified downstream processing structures **fail to fully leverage** the representational power. While self-supervised learning methods [18, 25] also succeed in capturing spatiotemporal heterogeneity by designing additional tasks, fully **end-to-end** joint optimization for spatiotemporal forecasting continues to present difficulties for these approaches. In short, the key drawbacks are: (1) reliance on auxiliary features; (2) high computational and memory costs; (3) failure to fully leverage captured heterogeneity; and (4) difficulties with end-to-end optimization.

To address the above limitations in prior works, we propose a novel **Heterogeneity-Informed Meta-Parameter Learning** scheme and a **Heterogeneity-Informed Meta-Network (HimNet)** for spatiotemporal time series forecasting. In detail, we first implicitly characterize heterogeneity by learning spatial and temporal embeddings from a clustering view. The representations gradually differentiate and form distinct clusters during training, capturing underlying spatiotemporal contexts. Next, a novel spatiotemporal meta-parameter learning paradigm is proposed to enhance model adaptability and generalizability, which is flexible for various domains. Specifically, we learn a unique parameter set for each spatiotemporal context via querying a small meta-parameter pool. Based on these, we further propose Heterogeneity-Informed Meta-Parameter Learning that uses the characterized heterogeneity to inform meta-parameter learning. Thus, our approach can not only capture but explicitly leverage spatiotemporal heterogeneity to improve forecasting. Finally, we design an end-to-end network called HimNet, implementing these techniques for spatiotemporal forecasting. In summary, our contributions are three-fold:

- Methodologically, we present a novel HimNet model for spatiotemporal time series forecasting. It captures inherent spatiotemporal heterogeneity through learnable embeddings, which then inform spatiotemporal meta-parameter learning to enhance model adaptability and generalizability.
- Theoretically, to the best of our knowledge, our proposed Heterogeneity-Informed Meta-Parameter Learning is the first method that not only captures but also fully leverages spatiotemporal heterogeneity. This enables our model to distinguish and adapt to different spatiotemporal contexts.
- Empirically, HimNet significantly outperforms state-of-the-art methods on five benchmarks based on extensive experiments, demonstrating superior performance with competitive efficiency. Visualization experiments further illustrate its strong interpretability through meta-parameters.

## 2 RELATED WORK

### 2.1 Spatiotemporal Forecasting

Spatiotemporal forecasting has seen extensive research as it plays a key role in many real-world applications [14, 15, 28, 38, 40, 66, 70, 71]. Early approaches relied on traditional time series analysis methods such as ARIMA [46] and VAR [54], as well as machine learning techniques including  $k$ -NN [10] and SVM [56], but they often fail to capture complex spatiotemporal dependencies inherent to the data. Recent years have witnessed remarkable progress in deep learning methods. Recurrent Neural Networks (RNNs) like LSTMs [43, 44] and GRUs [7] achieved performance gains by effectively modeling the temporal dynamics. Convolutional networks such as WaveNet [45] also found success via their long receptive fields. However, these models do not fully represent spatial dependencies critical to networked urban systems. To address this limitation, Graph Convolutional Networks (GCNs) have been extensively explored for spatiotemporal forecasting. Pioneering works such as STGCN [65] and DCRNN [37] achieved better performance by integrating GCNs with temporal models [2, 4, 60, 61]. Building on this foundation, many innovative methods have been proposed in recent years [12, 13, 29, 31, 34, 35, 50, 62]. Moreover, Transformer [57] has also revolutionized the field, motivating time series transformers [6, 58] that expertly capture spatiotemporal correlations [24, 27, 39, 67] or handle long sequences [41, 59, 68, 69]. While showing impressive performance, existing work still lacks further exploration of spatiotemporal heterogeneity. Our study aims to fill this gap through a novel HimNet that captures and leverages the heterogeneity for improved spatiotemporal forecasting.

### 2.2 Meta-Parameter Learning

One of the earliest works [49] proposed predicting network parameters for temporal modeling. More recently, Hypernetworks [21] applied this idea to recurrent networks by generating adaptive weights, acting as a form of weight-sharing across layers. Learnnet [3] was constructed as a second deep network to predict the parameters of another deep model. Dynamic Filter Networks [26] dynamically generate convolutional filters conditioned on input, increasing flexibility due to their adaptive nature. For meta multi-task learning, MetaMTL [5] introduced a shared Meta-LSTM to generate basic LSTM parameters based on the current input context.

In spatiotemporal applications, ST-GFSL [42] proposed learning non-shared parameters for cross-city transfer using learned spatiotemporal meta-knowledge from the input city. While effective in other domains, these methods were not designed specifically for spatiotemporal forecasting. To address this, recent works have introduced meta-parameter learning techniques for spatiotemporal data. ST-MetaNet [47] first applied meta-learning across spatial locations, using auxiliary POI and road network information as spatial meta-knowledge to learn multiple parameter sets. AGCRN [2] proposed node adaptive parameter learning to generate node-specific parameters from a learned embedding matrix, which can be interpreted as learning node specific patterns from a set of candidate patterns discovered from all spatiotemporal time series. ST-WA [8] proposes a spatiotemporal aware approach to jointly learn location-specific and time-varying model parameters from encoded stochastic variables. In contrast to these approaches, as shown in Table 1, HimNet learns meta-parameters using only the spatiotemporal time series itself, without depending on auxiliary features. Critically, we propose a concurrent learning scheme that operates on the temporal, spatial, and spatiotemporal joint dimensions simultaneously. Therefore, HimNet achieves maximum adaptability to any kind of spatiotemporal context. This makes our approach highly flexible and capable of extracting the full informational value from learned spatiotemporal heterogeneity.

**Table 1: Comparison of related meta-parameter learning methods for spatiotemporal forecasting.**

Method	Data-Independent	Temporal	Spatial	Joint
ST-MetaNet [47]	×	×	✓	×
AGCRN [2]	✓	×	✓	×
ST-WA [8]	✓	×	×	✓
<b>HimNet</b>	✓	✓	✓	✓

### 3 PROBLEM DEFINITION

Given a spatiotemporal time series  $X_{t-(T-1):t}$  over the past  $T$  time steps, our goal is to forecast the values over the future  $T'$  time steps. That is, we aim to map  $[X_{t-(T-1)}, \dots, X_t] \rightarrow [X_{t+1}, \dots, X_{t+T'}]$ , where each  $X_i \in \mathbb{R}^N$  represents the observations at the  $i$ -th time step for  $N$  time series, typically from sensors deployed at  $N$  locations.

### 4 METHODOLOGY

In this section, we present details of our proposed Heterogeneity-Informed Meta-parameter Learning scheme along with the HimNet model, where the key components are depicted in Figure 2. To better illustrate our proposed method, we consider a minibatch dimension  $B$  in the following discussions. For ease of understanding,  $B$  can be assumed to be 1 without loss of generality.

#### 4.1 Spatiotemporal Heterogeneity Modeling

A key aspect of modeling spatiotemporal heterogeneity is identifying and distinguishing input contexts across both temporal and spatial dimensions [11]. Rather than relying on auxiliary data [47, 53], we employ learnable embeddings [39, 52], which assign a unique representation to each spatiotemporal context.

For the temporal dimension, we construct a time-of-day embedding dictionary  $D_{tod} \in \mathbb{R}^{N_d \times d_{tod}}$  and a day-of-week dictionary  $D_{dow} \in \mathbb{R}^{N_w \times d_{dow}}$ , where  $d_{tod}$  and  $d_{dow}$  are the embedding dimensions,  $N_d$  denotes the number of timesteps per day, and  $N_w$  represents the number of days in a week. Given a minibatch of input samples  $X^b \in \mathbb{R}^{B \times T \times N}$  with historical length  $T$ , the last step's timestamp of each sample in the minibatch is used as the time index to extract the corresponding time-of-day embedding  $E_{tod} \in \mathbb{R}^{B \times d_{tod}}$  and day-of-week embedding  $E_{dow} \in \mathbb{R}^{B \times d_{dow}}$  from the dictionaries. The two embeddings are concatenated to obtain the overall temporal embedding  $E_t \in \mathbb{R}^{B \times d_t}$ :

$$E_t = E_{tod} || E_{dow}, \quad (1)$$

where  $d_t = d_{tod} + d_{dow}$  represents the temporal embedding dimension and  $||$  denotes concatenation operation. Time-of-day identifies periodic patterns with fine-grained time intervals, capturing phenomena like peak and off-peak hours. Day-of-week identifies meaningful longer-term patterns, such as the distinction in time series between weekdays and weekends. Leveraging these dictionaries, the temporal embedding aims to learn representations that can implicitly recognize and account for such temporal heterogeneity over multiple timescales.

For the spatial dimension, we utilize a spatial embedding matrix  $E_s \in \mathbb{R}^{N \times d_s}$ , where  $N$  denotes the total number of time series or spatial locations in the dataset (e.g. number of sensors) and  $d_s$  is the dimension of the embedding vector assigned to each location. Unlike the temporal dimension where the embeddings are extracted from learned dictionaries, here each of the  $N$  spatial locations is directly associated with a unique learnable spatial embedding vector initialized randomly in the embedding matrix. The goal of introducing  $E_s$  is to account for the inherent functional differences between locations that can influence time series patterns, such as factors related to infrastructure and urban design. It aims to learn latent representations that can help distinguish such diverse contexts, without the need for auxiliary geographical data. This facilitates modeling the spatial heterogeneity present in each location.

Furthermore, learning these embedding vectors essentially performs a dynamic clustering process. During model training, the representations within the embedding matrices gradually differentiate based on the input time series. Embedding vectors belonging to spatiotemporal contexts that exhibit similar trends in their time series will move closer in the latent space, and vice versa. As a result, this dynamic adjustment of the embeddings can be viewed as a clustering process, where representations organically form clusters. Each distinct cluster captures a typical context in the spatiotemporal time series. Analogous to the NLP models where the learned embeddings of "man" and "woman" can naturally be very close, this clustering process could be successfully achieved without involving any additional constraints like the way did in [25, 29]. This clustering perspective is what empowers the model to distinguish different contexts and thereby accurately model the heterogeneity across space and time. Through the learned embeddings, spatiotemporal heterogeneity is modeled in an intrinsic, data-driven manner, without requiring manual feature engineering or domain expertise to describe it in advance.

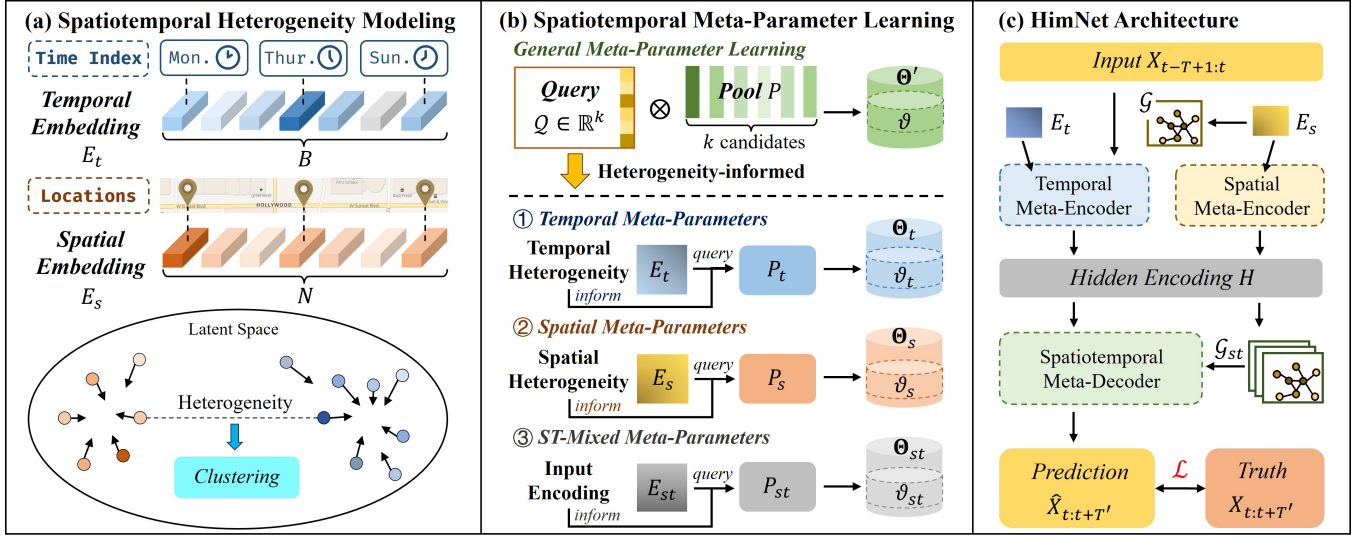


Figure 2: The overall illustration of the proposed Heterogeneity-Informed Meta-Parameter Learning and HimNet model.

## 4.2 Spatiotemporal Meta-Parameter Learning

To fully leverage the heterogeneity encoded in the spatiotemporal embeddings, we propose Heterogeneity-Informed Meta-Parameter Learning. It provides a simple yet effective way to improve model adaptability and generalizability.

We begin by introducing the general meta-parameter learning paradigm. For the model’s original parameter space  $\Theta$  with size  $S$ , our approach first extends it along a specific dimension to create an enlarged parameter space  $\Theta'$ . Specifically, we can build three enlarged spaces for the temporal and spatial dimensions: temporal parameter space  $\Theta_t \in \mathbb{R}^{\mathcal{T} \times S}$ , spatial parameter space  $\Theta_s \in \mathbb{R}^{N \times S}$ , and spatiotemporal joint space  $\Theta_{st} \in \mathbb{R}^{\mathcal{T} \times N \times S}$ . Here,  $\mathcal{T}$  represents the total number of timesteps and  $N$  is the number of spatial locations in the dataset. This extension aims to assign a unique parameter set to each spatiotemporal context, rather than sharing  $\Theta$ . Directly optimizing these enlarged parameter spaces is prohibitively expensive, as they become very huge, especially when  $\mathcal{T}$  and  $N$  are large, which will lead to exploding computational and memory costs. To address this challenge, we maintain a small meta-parameter pool for each parameter space, which contains  $k$  parameter candidates. The pool size  $k$  is defined to be much smaller than  $\mathcal{T}$  and  $N$ , but sufficiently large to encapsulate the variety of different contexts. For an incoming query representing a specific spatiotemporal context, we dynamically generate its meta-parameter as a weighted combination of the pool candidates.

For a meta-parameter pool  $P \in \mathbb{R}^{k \times S}$ , given a query  $Q \in \mathbb{R}^k$ , the general formulation of our meta-parameter learning paradigm is:

$$\vartheta = Q \cdot P, \quad (2)$$

where  $\vartheta \in \mathbb{R}^S$  is the generated meta-parameter. By maintaining meta-parameter pools, our approach alleviates this computational burden by optimizing within the compact pools rather than the full enlarged parameter spaces. Thus, the complexity is reduced from  $O(\mathcal{T}N)$  to  $O(k)$ , where  $k \ll \mathcal{T}N$ . This makes the learning computationally feasible for large spatiotemporal datasets.

Specifically, we leverage the embeddings proposed earlier that encode spatiotemporal heterogeneity as queries to adaptively generate the meta-parameters for each spatiotemporal context. This results in a **Heterogeneity-Informed Meta-Parameter Learning** approach. Based on Equation 2, three types of meta-parameters are generated for the respective enlarged parameter spaces.

**Temporal Meta-Parameters.** We maintain a small temporal meta-parameter pool  $P_t \in \mathbb{R}^{d_t \times S}$  containing  $d_t$  candidates. Using the temporal embedding  $E_t \in \mathbb{R}^{B \times d_t}$  as queries, the temporal meta-parameters  $\vartheta_t \in \mathbb{R}^{B \times S}$  are generated by:

$$\vartheta_t = E_t \cdot P_t. \quad (3)$$

**Spatial Meta-Parameters.** We maintain a small spatial meta-parameter pool  $P_s \in \mathbb{R}^{d_s \times S}$  with  $d_s$  candidates. Using the spatial embedding  $E_s \in \mathbb{R}^{N \times d_s}$  as queries, the spatial meta-parameters  $\vartheta_s \in \mathbb{R}^{N \times S}$  for each location are generated by:

$$\vartheta_s = E_s \cdot P_s. \quad (4)$$

**ST-Mixed Meta-Parameters.** To directly create a joint spatiotemporal embedding is prohibitive, as its size would also be too large to optimize effectively. Instead, we utilize the rich information inherently contained within the input data itself [8], where the time series patterns naturally reflect spatiotemporal heterogeneity. For a minibatch of input samples  $X^b \in \mathbb{R}^{B \times \mathcal{T} \times N}$ , we encode it into a spatiotemporal embedding  $E_{st} \in \mathbb{R}^{B \times N \times d_{st}}$  as:

$$E_{st} = F_{enc}(X^b), \quad (5)$$

where  $d_{st}$  is the embedding dimension, and  $F_{enc}(\cdot)$  represents an encoding function such as linear projection, TCN [65], or GRU [37] designed to encode the input into a hidden representation.

Accordingly, we maintain a spatiotemporal meta-parameter pool  $P_{st} \in \mathbb{R}^{d_{st} \times S}$  having  $d_{st}$  candidates. Leveraging the encoded spatiotemporal embedding  $E_{st}$  as queries, the spatiotemporal-mixed (ST-mixed) meta-parameters  $\vartheta_{st} \in \mathbb{R}^{B \times N \times S}$  are generated by:

$$\vartheta_{st} = E_{st} \cdot P_{st}. \quad (6)$$

While we generate the meta-parameters based on the proposed embeddings, the underlying meta-parameter learning technique itself is not limited specifically to these embeddings. We present a purely data-driven approach using only the intrinsic spatiotemporal heterogeneity in the time series itself. However, other auxiliary spatiotemporal features could also be utilized if available in the dataset, such as POIs, weather patterns, or urban structural characteristics. These supplemental contextual attributes could be encoded into the query representation to provide further instruction for meta-parameter learning. Therefore, the method is flexible and can leverage diverse contextual features to learn improved meta-parameters tailored to various application domains.

### 4.3 Heterogeneity-Informed Spatiotemporal Meta-Network

Leveraging our proposed techniques, we implement an end-to-end model called Heterogeneity-Informed Spatiotemporal Meta-Network (HimNet) for accurate spatiotemporal forecasting.

Taking inspiration from GCNs, researchers have developed graph convolutional recurrent networks [37, 50, 64] which leverage both graph convolutions and recurrent transformations. By integrating graph convolutions within recurrent cells, these models can effectively capture temporal dynamics while also accounting for the spatial relations in the graph. Therefore, our proposed HimNet architecture uses variants of the widely adopted Graph Convolutional Recurrent Unit (GCRU) [2, 29] as the fundamental building block. GCRU is formulated by:

$$\begin{aligned} r_t &= \sigma(\Theta_r \star_{\mathcal{G}} [X_t, H_{t-1}] + b_r) \\ u_t &= \sigma(\Theta_u \star_{\mathcal{G}} [X_t, H_{t-1}] + b_u) \\ c_t &= \tanh(\Theta_c \star_{\mathcal{G}} [X_t, (r_t \odot H_{t-1})] + b_c) \\ H_t &= u_t \odot H_{t-1} + (1 - u_t) \odot c_t, \end{aligned} \quad (7)$$

where  $X_t \in \mathbb{R}^N$  and  $H_t \in \mathbb{R}^{N \times h}$  denote the input and output at timestep  $t$ .  $h$  is the hidden size.  $r_t$  and  $u_t$  are the reset and update gates.  $\Theta_r, \Theta_u, \Theta_c$  are parameters for the corresponding filters in the graph convolution operation  $\star_{\mathcal{G}}$ , which is defined as:

$$Z = U \star_{\mathcal{G}} = \sum_{k=0}^K \tilde{A} U W_k, \quad (8)$$

where  $U \in \mathbb{R}^{N \times C}$  is the input,  $Z \in \mathbb{R}^{N \times h}$  is the output, and  $C$  denotes the input channels.  $\tilde{A}$  represents the topology of graph  $\mathcal{G}$ , and  $W \in \mathbb{R}^{K \times C \times h}$  is the kernel parameter  $\Theta$ .

By applying temporal meta-parameter learning to GCRU, we propose a **temporal meta-encoder**. Referring to Equation 3, the generated temporal meta-parameters in this encoder take the form  $W_t \in \mathbb{R}^{B \times K \times C \times h}$ . Similarly, we build a **spatial meta-encoder** via spatial meta-parameter learning, with generated spatial meta-parameters  $W_s \in \mathbb{R}^{N \times K \times C \times h}$  by applying Equation 4. For the graph  $\mathcal{G}$  used in the encoders, rather than relying on a static pre-defined adjacency matrix as in prior works [19, 37, 65], we follow the adaptive graph learning design [60, 61]. Specifically, we leverage our learned spatial embeddings  $E_s$  to dynamically generate the adjacency matrix  $\tilde{A} \in \mathbb{R}^{N \times N}$  as:

$$\tilde{A} = \text{Softmax}(\text{ReLU}(E_s \cdot E_s^T)). \quad (9)$$

In short, given an input  $X^b \in \mathbb{R}^{B \times T \times N}$ , the two encoders operate in parallel to encode it into two hidden representations based on their respective meta-parameters. These representations are then summed to yield the final combined hidden encoding  $H \in \mathbb{R}^{B \times N \times h}$ .

To decode the latent representation  $H$  into predictions, we propose a **spatiotemporal meta-decoder** that leverages ST-mixed meta-parameters. Specifically, we first generate the corresponding spatiotemporal embedding  $E_{st} \in \mathbb{R}^{B \times N \times d_{st}}$  from  $H$ :

$$E_{st} = H \cdot W_E + b_E, \quad (10)$$

where  $W_E \in \mathbb{R}^{h \times d_{st}}$  and  $b_E \in \mathbb{R}^{d_{st}}$  are the linear projection parameters. According to Equation 6, we then produce the ST-mixed meta-parameters for GCRU as  $W_{st} \in \mathbb{R}^{B \times N \times K \times C \times h}$  using query  $E_{st}$ . Moreover, inspired by [29], we apply a time-varying adaptive graph  $\mathcal{G}_{st}$  inferred from  $E_{st}$ :

$$\tilde{A}_{st} = \text{Softmax}(\text{ReLU}(E_{st} \cdot E_{st}^T)), \quad (11)$$

where  $\tilde{A}_{st} \in \mathbb{R}^{B \times N \times N}$ . The decoder takes the initial hidden state from  $H$  and iteratively generates predictions  $\hat{X}$  for each future timestep by applying the GCRU cell parameterized by  $W_{st}$ .

Given ground truth  $X_{t+1:t+T'}$ , we mainly adopt the Mean Absolute Error (MAE) loss as our training objective to optimize multi-step predictions jointly. The loss function for HimNet's multi-step spatiotemporal time series forecasting can be formulated as:

$$\mathcal{L} = \text{MAE}(\hat{X}_{t+1:t+T'}, X_{t+1:t+T'}) = \frac{1}{T'N} \sum_{i=1}^{T'} \sum_{j=1}^N |\hat{X}_{i,j} - X_{i,j}|. \quad (12)$$

## 5 EXPERIMENT

### 5.1 Experimental Setup

**Datasets.** Our proposed model is evaluated on the **five most commonly used** spatiotemporal forecasting benchmarks. The METRLA dataset and PEMS BAY dataset [37] contain traffic speed data recorded by traffic sensors in Los Angeles and the Bay Area, respectively. The PEMS04, PEMS07, and PEMS08 datasets [53] are three traffic flow datasets collected from the California Transportation Performance Management System (PeMS). The raw data has a fine temporal granularity of 5 minutes between consecutive timesteps. Therefore,  $N_d=288$  and  $N_w=7$  in these benchmarks. Additional details regarding the five benchmarks can be found in Table 2. As part of data preprocessing, we perform Z-score normalization on the raw inputs to rescale the data to have zero mean and unit variance. To ensure a fair comparison to previous methods, we adopt the commonly used dataset divisions from prior works. For the METRLA and PEMS BAY datasets, we use 70% of the data for training, 10% for validation, and

Table 2: Summary of datasets.

Dataset	#Sensors	#Timesteps	Time Range
METRLA	207	34,272	03/2012 - 06/2012
PEMSBAY	325	52,116	01/2017 - 05/2017
PEMS04	307	16,992	01/2018 - 02/2018
PEMS07	883	28,224	05/2017 - 08/2017
PEMS08	170	17,856	07/2016 - 08/2016

**Table 3: Performance on METRLA, PEMS04, PEMS07, and PEMS08 datasets.**

Dataset	Metric	HI	GRU	STGCN	DCRNN	GWNet	AGCRN	GTS	STNorm	STID	ST-WA	PDFormer	MegaCRN	HimNet	
METRLA	Step 3 15 min	MAE	6.80	3.07	2.75	2.67	2.69	2.85	2.75	2.81	2.82	2.89	2.83	2.65	<b>2.60</b>
		RMSE	14.21	6.09	5.29	5.16	5.15	5.53	5.27	5.57	5.53	5.62	5.45	5.08	<b>5.02</b>
		MAPE	16.72%	8.14%	7.10%	6.86%	6.99%	7.63%	7.12%	7.40%	7.75%	7.66%	7.77%	6.73%	<b>6.70%</b>
	Step 6 30 min	MAE	6.80	3.77	3.15	3.12	3.08	3.20	3.14	3.18	3.19	3.25	3.20	3.04	<b>2.95</b>
		RMSE	14.21	7.69	6.35	6.27	6.20	6.52	6.33	6.59	6.57	6.61	6.46	6.18	<b>6.06</b>
		MAPE	16.72%	10.71%	8.62%	8.42%	8.47%	9.00%	8.62%	8.47%	9.39%	9.22%	9.19%	8.22%	<b>8.11%</b>
	Step 12 60 min	MAE	6.80	4.88	3.60	3.54	3.51	3.59	3.59	3.57	3.55	3.68	3.62	3.51	<b>3.37</b>
		RMSE	14.21	9.75	7.43	7.47	7.28	7.45	7.44	7.51	7.55	7.59	7.47	7.39	<b>7.22</b>
		MAPE	16.71%	14.91%	10.35%	10.32%	9.96%	10.47%	10.25%	10.24%	10.95%	10.78%	10.91%	10.01%	<b>9.79%</b>
PEMSBAY	Step 3 15 min	MAE	3.05	1.44	1.36	1.31	1.30	1.35	1.37	1.33	1.31	1.37	1.32	1.28	<b>1.27</b>
		RMSE	7.03	3.15	2.88	2.76	2.73	2.88	2.92	2.82	2.79	2.88	2.83	2.71	<b>2.68</b>
		MAPE	6.85%	3.01%	2.86%	2.73%	2.71%	2.91%	2.85%	2.76%	2.78%	2.86%	2.78%	2.67%	<b>2.64%</b>
	Step 6 30 min	MAE	3.05	1.97	1.70	1.65	1.63	1.67	1.72	1.65	1.64	1.70	1.64	1.60	<b>1.57</b>
		RMSE	7.03	4.60	3.84	3.75	3.73	3.82	3.86	3.77	3.73	3.81	3.79	3.69	<b>3.60</b>
		MAPE	6.84%	4.45%	3.79%	3.71%	3.73%	3.81%	3.88%	3.66%	3.73%	3.81%	3.71%	3.60%	<b>3.52%</b>
	Step 12 60 min	MAE	3.05	2.70	2.02	1.97	1.99	1.94	2.06	1.92	1.91	2.00	1.91	1.90	<b>1.84</b>
		RMSE	7.01	6.28	4.63	4.60	4.60	4.50	4.60	4.45	4.42	4.52	4.43	4.49	<b>4.32</b>
		MAPE	6.83%	6.72%	4.72%	4.68%	4.71%	4.55%	4.88%	4.46%	4.55%	4.63%	4.51%	4.53%	<b>4.33%</b>
PEMS04	Average	MAE	42.35	25.55	19.57	19.63	18.53	19.38	20.96	18.96	18.38	19.06	18.36	18.72	<b>18.14</b>
		RMSE	61.66	39.71	31.38	31.26	29.92	31.25	32.95	30.98	29.95	31.02	30.03	30.53	<b>29.88</b>
		MAPE	29.92%	17.35%	13.44%	13.59%	12.89%	13.40%	14.66%	12.69%	12.04%	12.52%	12.00%	12.77%	<b>12.00%</b>
PEMS07	Average	MAE	49.29	26.74	21.74	21.16	20.47	20.57	22.15	20.50	19.61	20.74	19.97	19.83	<b>19.21</b>
		RMSE	71.34	42.78	35.27	34.14	33.47	34.40	35.10	34.66	32.79	34.05	32.95	32.91	<b>32.75</b>
		MAPE	22.75%	11.58%	9.24%	9.02%	8.61%	8.74%	9.38%	8.75%	8.30%	8.77%	8.55%	8.36%	<b>8.03%</b>
PEMS08	Average	MAE	34.66	19.36	16.08	15.22	14.40	15.32	16.49	15.41	14.21	15.41	13.58	14.75	<b>13.57</b>
		RMSE	50.45	31.20	25.39	24.17	23.39	24.41	26.08	24.77	23.28	24.62	23.41	23.73	<b>23.22</b>
		MAPE	21.63%	12.43%	10.60%	10.21%	9.21%	10.03%	10.54%	9.76%	9.27%	9.94%	9.05%	9.48%	<b>8.98%</b>

the remaining 20% for testing [37, 61]. In the case of the PEMS04, PEMS07, and PEMS08 datasets, we divide them into 60%, 20%, and 20%, respectively [19, 39]. In this study, we ensured **the ethical use** of these five publicly available datasets.

**Settings.** We performed hyper-parameter search on each dataset. The encoder and decoder each contain one layer  $L=1$  with a hidden dimension  $h=64$  for the first four datasets, and  $h=96$  for the PEMS08 dataset. For the embeddings, the dimensions of the temporal embedding  $d_t$ , the spatial embedding  $d_s$ , and the spatiotemporal embedding  $d_{st}$  are all set to 16 for the first four datasets. And for PEMS08, the dimensions are 12, 14, and 10, respectively. The input and prediction horizons are both set to 1 hour ( $T=T'=12$  timesteps). We use the Adam optimizer with an initial learning rate of 0.001 and decay over training, and the batch size  $B$  is 16. The maximum training epochs is 200, with an early stop patience set to 20. For the loss function, we employ MAE loss for METRLA and PEMS-BAY. For PEMS04, PEMS07, and PEMS08, we further employ Huber loss [23], a variant of MAE that is more robust. Model performance is evaluated using MAE, Root Mean Square Error (RMSE), and Mean Absolute Percentage Error (MAPE). All following experiments are conducted on NVIDIA GeForce RTX 3090 GPUs.

**Baselines.** We compare our HimNet to several widely adopted baselines. HI [9] is a standard statistical technique. GRU [7] is a widely adopted univariate time series forecasting method. As for

spatiotemporal forecasting, we select several typical models including STGCN [65], DCRNN [37], Graph WaveNet [61], AGCRN [2], GTS [50], STNorm [11], STID [52], ST-WA [8], PDFormer [27] and MegaCRN [29]. Among them, DCRNN, GTS, and MegaCRN also apply GCRU-based architectures. AGCRN and ST-WA are meta-parameter learning methods closely related to our approach.

## 5.2 Performance Evaluation

The comparison results for the performance of spatiotemporal forecasting are given in Table 3. For the METRLA and PEMS04 datasets, we report performance on 3, 6, and 12 timesteps (15, 30, and 60 minutes). Consistent with previous works, we report the average performance over all 12 predicted timesteps for the PEMS04, PEMS07, and PEMS08 datasets. From the results, we obtain the following observations: (1) Our proposed model, HimNet, significantly outperforms all baselines across all metrics and datasets, demonstrating the effectiveness of our method. By learning meta-parameters based on spatiotemporal heterogeneity, our approach is better able to adapt to diverse spatiotemporal contexts for accurate forecasting. (2) Compared with other GCRU-based models DCRNN, GTS, and MegaCRN, HimNet achieves better performance, highlighting the superiority of our meta-parameter learning scheme. (3) While AGCRN learns parameters only for each spatial node, our method further considers the temporal dimension and utilizes spatiotemporal heterogeneity. ST-WA learns specific parameters for

each location and timestep based only on the knowledge learned from the current input. However, our method fully captures and leverages the global spatiotemporal heterogeneity, providing important guidance for more precise local parameter learning. As a result, our HimNet demonstrates better forecasting performance than others.

### 5.3 Ablation Study

In this section, we conduct ablation studies to validate key components of our proposed approach. We designed the following variants: (1) w/o  $E_t$ : replaces the temporal embedding with a static matrix of all ones, thus removing temporal heterogeneity modeling. (2) w/o  $E_s$ : replaces the spatial embedding with a static matrix of all ones, thus removing spatial heterogeneity modeling. (3) w/o  $E_{st}$ : replaces the spatiotemporal embedding with a static matrix of all ones. (4) w/o TMP: removes temporal meta-parameters by downgrading to randomly initialized parameters. (5) w/o SMP: removes spatial meta-parameters. (6) w/o STMP: removes ST-mixed meta-parameters. As shown in Table 4, using identical queries decreases forecasting performance, demonstrating the effectiveness of our heterogeneity-informed approach. Moreover, removing meta-parameters leads to more substantial performance degradation, highlighting the value of applying the spatiotemporal meta-parameters modulated by our method. All these validate that HimNet is complete and indivisible to achieve superior spatiotemporal forecasting performance.

**Table 4: Average MAE of the ablated variants of HimNet.**

Model	METRLA	PEMSBAY	PEMS04	PEMS07	PEMS08
w/o $E_t$	2.94	1.53	18.35	22.00	14.14
w/o $E_s$	3.49	1.74	21.30	19.26	14.79
w/o $E_{st}$	3.07	1.55	18.55	19.77	13.61
w/o TMP	2.94	1.54	18.65	19.58	14.44
w/o SMP	3.53	1.75	21.41	22.26	14.07
w/o STMP	3.01	1.57	18.65	19.86	13.72
<b>HimNet</b>	<b>2.92</b>	<b>1.51</b>	<b>18.14</b>	<b>19.21</b>	<b>13.57</b>

### 5.4 Hyper-Parameter Study

We conduct experiments on our model’s sensitivity to key hyper-parameters, including the dimension of the temporal embedding  $d_t$ , the spatial embedding  $d_s$ , and the spatiotemporal embedding  $d_{st}$ . Figure 3 plots the average RMSE of predictions on the METRLA dataset when varying each embedding dimension from 4 to 24. Interestingly, we find that our model is fairly robust to changes in

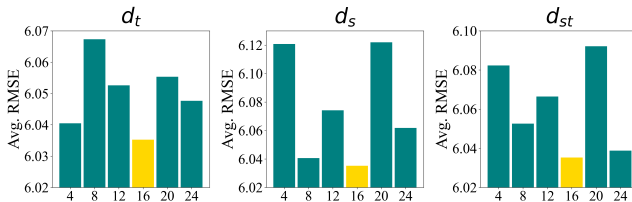


**Figure 3: RMSE w.r.t. embedding dimensions on METRLA.**

these hyper-parameters. Across the ranges tested, the RMSE difference between the best and worst-performing configurations is only approximately 0.1. An embedding size of 16 generally provides good results with a tractable parameter size. Still, some trends emerge where decreasing a dimension too much begins to exhibit signs of under-fitting, while larger dimensions will substantially increase parameter size but without notable improvement in performance.

### 5.5 Efficiency Study

We evaluate efficiency by comparing HimNet with 10 spatiotemporal baseline models. Table 5 reports the number of parameters, per-batch runtime, per-epoch runtime, and GPU memory usage on METRLA (batch size  $B=16$ ).

As shown in the table, models using TCNs, such as STGCN, GWNet and STNorm, perform relatively well because of the high computational efficiency of convolution. In comparison, the next four models with GCRU architecture show a notable efficiency gap due to the iterative nature of RNNs that intrinsically presents a disadvantage. Additionally, Transformer-based models like ST-WA and PDFormer are even worse due to their quadratic computational complexity. Among these, STID performs best as its backbone is simply linear layers. We also observe that HimNet’s memory usage is relatively high, because our design of the meta-parameter pools will enlarge its parameter size. In summary, our HimNet achieves decent efficiency compared with other GCRU-based models, and outperforms the Transformer-based baselines.

We further analyze a variant HimNet- $\Theta'$  that removes meta-parameter pools and directly optimizes the three enlarged parameter spaces. HimNet- $\Theta'$  contains over 10.9 billion parameters, unavailable on any GPUs we can get. This is consistent with our analysis that directly optimizing the enlarged parameter spaces leads to intractable memory costs, which validates the necessity of our meta-parameter pool design to maintain efficiency while enabling flexible parameterization.

**Table 5: Efficiency comparison on METRLA dataset.**

Model	#Params	Time / Batch	Time / Epoch	Mem Usage
STID [52]	118K	8ms	12s	1420MB
STGCN [65]	246K	23ms	34s	1650MB
GWNet [61]	309K	40ms	60s	1994MB
STNorm [11]	224K	39ms	59s	1818MB
DCRNN [37]	372K	189ms	284s	2134MB
AGCRN [2]	752K	54ms	82s	2492MB
GTS [50]	38.5M	114ms	171s	4096MB
MegaCRN [29]	389K	89ms	134s	1962MB
ST-WA [8]	375K	135ms	203s	2668MB
PDFormer [27]	531K	173ms	260s	6938MB
HimNet- $\Theta'$	10.9B	N/A	N/A	N/A
<b>HimNet</b>	1251K	97ms	144s	6056MB

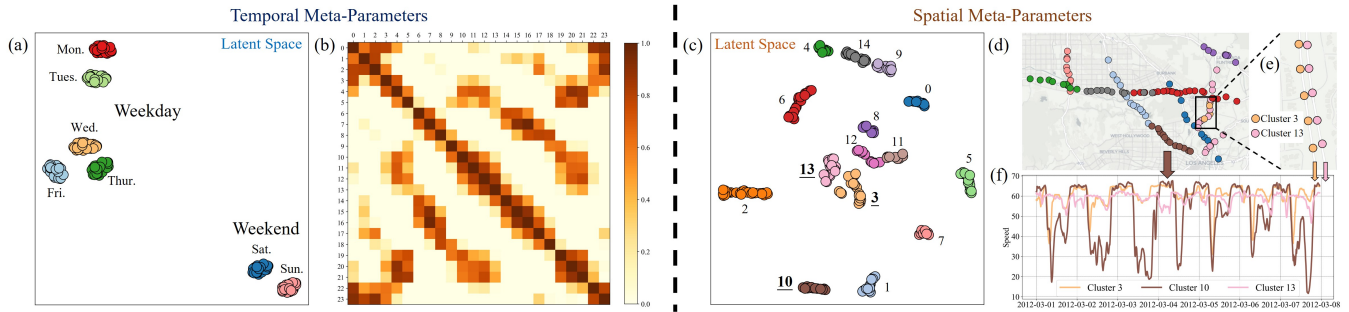


**Figure 4: t-SNE visualization of the temporal and spatial meta-parameters. (a): Visualization for each day in a week where every cluster contains 24 points representing each hour’s temporal meta-parameter. (b): The cosine similarity matrix of the meta-parameters across 24 hours in a day. (c): Visualization for each sensor’s spatial meta-parameter in METRLA dataset. (d): Sensor points in (c) plotted on map, with only one lane of points shown for dual carriageways. (e): Clusters 3 and 13 are located on opposite lanes of the same road. (f): The one-week time series of clusters 3, 10, and 13.**

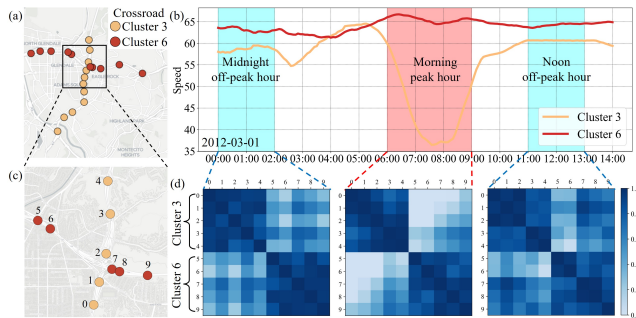


**Figure 5: The evolving ST-mixed meta-parameters. (a): Distribution of clusters 3 and 6 around a crossroad area. (b): The traffic speed time series of the two clusters at peak hour and off-peak hour. (c): A closer view of 10 sensors at the crossroad. (d): The cosine similarity of their ST-mixed meta-parameters across three time periods.**

## 5.6 Case Study

In this section, we analyze the learned meta-parameters through visualizations to gain better interpretability and demonstrate how they reflect meaningful circumstances in the real world.

**Temporal Meta-Parameters.** Figure 4 provides visualizations on temporal and spatial meta-parameters based on t-SNE [55] dimensionality reduction. We extract the temporal meta-parameters for each hour across the days of a week. With one day sampled at an hourly granularity, this results in a total of 168 data points embedded in the 2D latent space. As shown in Figure 4(a), distinct tight clusters form for each individual day, demonstrating our method’s ability to differentiate days of the week. Notably, weekdays and weekends are widely separated, underscoring our effectiveness in capturing the temporal heterogeneity between these day types. Figure 4(b) shows the cosine similarity between the temporal meta-parameters of each hourly interval within a day. Higher similarity is observed between adjacent hours, decreasing with increased temporal distance as expected. Interestingly, the time periods when people travel frequently exhibit high similarity. For example, the periods

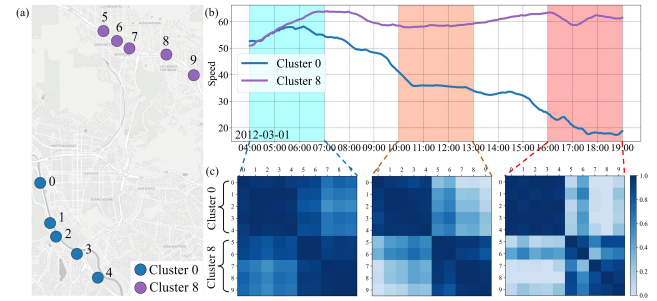


**Figure 6: The evolving ST-mixed meta-parameters of clusters 0 and 8. As the time series diverge, they evolve accordingly.**

between 6-9am and 4-7pm show increased similarity, reflecting real-world commuting behaviors. These examples demonstrate that our proposed method successfully identifies and distinguishes the diverse temporal contexts associated with different time periods.

**Spatial Meta-Parameters.** For the spatial meta-parameters, we analyze the METRLA dataset as a case study. It contains 207 sensor locations whose spatial meta-parameters are embedded in 2D latent space as shown in Figure 4(c). The 207 points naturally form into 15 clusters marked with different colors. To interpret these clusters, we draw them onto a real map of Los Angeles in Figure 4(d). Remarkably, each cluster precisely aligns with road segments, underscoring our models’ strong power to capture real-world urban structural characteristics, even without the help of graph topology. Moreover, opposite lanes of the same road contain points from different clusters. Figure 4(e) shows clusters 3 and 13 as an example. For visual clarity, we manually select one lane per road to draw Figure 4(d). This exact matching between learned clusters and real road topology demonstrates our method’s ability to explicitly distinguish spatial heterogeneity. Furthermore, we analyze the time series of clusters 3, 10, and 13 specifically. Cluster 10 corresponds to a major downtown road prone to severe congestion. Clusters 3 and 13 are located on the opposite lanes of a minor road. As expected, their traffic speed time series in Figure 4(f) show that clusters 3 and 13 are closely matched while significantly differing from 10,



consistent with our observations on the map and the latent space in Figure 4(c). This validates that the spatial meta-parameters encode meaningful contexts reflecting spatial heterogeneity.

**ST-Mixed Meta-Parameters.** Figure 5 provides a case study of the evolving ST-mixed meta-parameters. Clusters 3 and 6 from the crossroad area in Figure 5(a) are analyzed. Their traffic speed time series are shown in Figure 5(b) with three periods highlighted: midnight off-peak, morning peak, and noon off-peak. Ten nearby sensors (5 per cluster) on the crossroad are visualized in Figure 5(c). For their ST-mixed parameters, we draw cosine similarity heatmaps across the three time periods in Figure 5(d). As expected, within-cluster similarity is generally higher than cross-cluster similarity. In detail, during midnight off-peak hours, both clusters exhibit similar traffic speed patterns, reflected by high cross-cluster similarity. However, during the morning peak, cluster 3 shows a sharp drop in speed while cluster 6 maintains a higher level. Their time series diverge, resulting in lower cross-cluster similarity. At noon, the speed patterns in both clusters become closer, leading to an increase in cross-cluster similarity again. Moreover, in Figure 6, we conduct another case study on clusters 0 and 8. Figure 6(a) shows five sensors each selected from the two clusters. As shown in Figure 6(b), their time series diverge substantially over time. Correspondingly, as illustrated in Figure 6(c), the cross-cluster similarity between the ST-mixed meta-parameters associated with each sensor decreases accordingly over the three selected time periods. These case studies intuitively explain how our ST-mixed meta-parameters evolve spatially and temporally. Thus, the proposed approach has strong adaptability to various spatiotemporal contexts, with meta-parameters accurately capturing changes between different time periods for each location. Furthermore, this also confirms the power of our method to jointly model spatiotemporal heterogeneity.

## 6 CONCLUSION

In this study, we proposed a novel **Heterogeneity-Informed Meta-Parameter Learning** scheme along with the state-of-the-art Heterogeneity-Informed Spatiotemporal Meta-Network (**HimNet**) for spatiotemporal forecasting. In detail, we captured spatiotemporal heterogeneity by learning spatial and temporal embeddings. A novel meta-parameter learning paradigm was proposed to learn spatiotemporal-specific parameters from meta-parameter pools. Critically, our proposed approach can fully leverage the captured spatiotemporal heterogeneity to inform meta-parameter learning. Extensive experiments on five benchmarks demonstrated HimNet's superior performance. Further visualization analyses on meta-parameters revealed its strong interpretability.

## ACKNOWLEDGMENT

This work was partially supported by the grants of National Key Research and Development Project (2021YFB1714400) of China, Jilin Provincial International Cooperation Key Laboratory for Super Smart City and Zhujiang Project (2019QN01S744).

## REFERENCES

[1] Rafal A Angryk, Petrus C Martens, Berkay Aydin, Dustin Kempton, Sushant S Mahajan, Sunitha Basodi, Azim Ahmadzadeh, Xumin Cai, Soukaina Filali Boubrahimi, Shah Muhammad Hamdi, et al. 2020. Multivariate time series dataset for space weather data analytics. *Scientific data* 7, 1 (2020), 227.

[2] Lei Bai, Lina Yao, Can Li, Xianzhi Wang, and Can Wang. 2020. Adaptive graph convolutional recurrent network for traffic forecasting. *Advances in neural information processing systems* 33 (2020), 17804–17815.

[3] Luca Bertinetto, João F Henriques, Jack Valmadre, Philip Torr, and Andrea Vedaldi. 2016. Learning feed-forward one-shot learners. *Advances in neural information processing systems* 29 (2016).

[4] Defu Cao, Yujing Wang, Juanyong Duan, Ce Zhang, Xia Zhu, Congrui Huang, Yunhai Tong, Bixiong Xu, Jing Bai, Jie Tong, et al. 2020. Spectral temporal graph neural network for multivariate time-series forecasting. *Advances in neural information processing systems* 33 (2020), 17766–17778.

[5] Junkun Chen, Xipeng Qiu, Pengfei Liu, and Xuanjing Huang. 2018. Meta multi-task learning for sequence modeling. In *Proceedings of the AAAI Conference on Artificial Intelligence*, Vol. 32.

[6] Peng Chen, Yingying Zhang, Yunyao Cheng, Yang Shu, Yihang Wang, Qingsong Wen, Bin Yang, and Chenjuan Guo. 2024. Multi-scale Transformers with Adaptive Pathways for Time Series Forecasting. In *International Conference on Learning Representations*.

[7] Junyoung Chung, Caglar Gulcehre, KyungHyun Cho, and Yoshua Bengio. 2014. Empirical evaluation of gated recurrent neural networks on sequence modeling. *arXiv preprint arXiv:1412.3555* (2014).

[8] Razvan-Gabriel Cirstea, Bin Yang, Chenjuan Guo, Tung Kieu, and Shirui Pan. 2022. Towards Spatio-Temporal Aware Traffic Time Series Forecasting—Full Version. *arXiv preprint arXiv:2203.15737* (2022).

[9] Yue Cui, Jiandong Xie, and Kai Zheng. 2021. Historical inertia: A neglected but powerful baseline for long sequence time-series forecasting. In *Proceedings of the 30th ACM International Conference on Information & Knowledge Management*. 2965–2969.

[10] Gary A Davis and Nancy L Nihan. 1991. Nonparametric regression and short-term freeway traffic forecasting. *Journal of Transportation Engineering* 117, 2 (1991), 178–188.

[11] Jinliang Deng, Xiusi Chen, Renhe Jiang, Xuan Song, and Ivor W Tsang. 2021. St-norm: Spatial and temporal normalization for multi-variate time series forecasting. In *Proceedings of the 27th ACM SIGKDD conference on knowledge discovery & data mining*. 269–278.

[12] Jinliang Deng, Xiusi Chen, Renhe Jiang, Xuan Song, and Ivor W Tsang. 2022. A multi-view multi-task learning framework for multi-variate time series forecasting. *IEEE Transactions on Knowledge and Data Engineering* (2022).

[13] Jinliang Deng, Xiusi Chen, Renhe Jiang, Du Yin, Yi Yang, Xuan Song, and Ivor W Tsang. 2024. Disentangling Structured Components: Towards Adaptive, Interpretable and Scalable Time Series Forecasting. *IEEE Transactions on Knowledge and Data Engineering* (2024).

[14] Jiewen Deng, Jinliang Deng, Renhe Jiang, and Xuan Song. 2023. Learning Gaussian mixture representations for tensor time series forecasting. In *Proceedings of the Thirty-Second International Joint Conference on Artificial Intelligence*.

[15] Jiewen Deng, Renhe Jiang, Jiaqi Zhang, and Xuan Song. 2024. Multi-Modality Spatio-Temporal Forecasting via Self-Supervised Learning. *arXiv preprint arXiv:2405.03255* (2024).

[16] Yuchen Fang, Yanjun Qin, Haiyong Luo, Fang Zhao, Bingbing Xu, Liang Zeng, and Chenxing Wang. 2023. When spatio-temporal meet wavelets: Disentangled traffic forecasting via efficient spectral graph attention networks. In *2023 IEEE 39th International Conference on Data Engineering (ICDE)*. IEEE, 517–529.

[17] Zheng Fang, Qingqing Long, Guojie Song, and Kunqing Xie. 2021. Spatial-temporal graph ode networks for traffic flow forecasting. In *Proceedings of the 27th ACM SIGKDD Conference on Knowledge Discovery & Data Mining*. 364–373.

[18] Haotian Gao, Renhe Jiang, Zheng Dong, Jinliang Deng, and Xuan Song. 2023. Spatio-Temporal-Decoupled Masked Pre-training for Traffic Forecasting. *arXiv preprint arXiv:2312.00516* (2023).

[19] Shengnan Guo, Youfang Lin, Ning Feng, Chao Song, and Huaiyu Wan. 2019. Attention based spatial-temporal graph convolutional networks for traffic flow forecasting. In *Proceedings of the AAAI conference on artificial intelligence*, Vol. 33. 922–929.

[20] Mridul Gupta, Hariprasad Kodamana, and Sayan Ranu. 2023. FRIGATE: Frugal Spatio-temporal Forecasting on Road Networks. *arXiv preprint arXiv:2306.08277* (2023).

[21] David Ha, Andrew M Dai, and Quoc V Le. 2016. HyperNetworks. In *International Conference on Learning Representations*.

[22] Liangzhe Han, Bowen Du, Leilei Sun, Yanjie Fu, Yisheng Lv, and Hui Xiong. 2021. Dynamic and Multi-faceted Spatio-temporal Deep Learning for Traffic Speed Forecasting. In *Proceedings of the 27th ACM SIGKDD Conference on Knowledge Discovery & Data Mining*. 547–555.

[23] Peter J Huber. 1964. Robust Estimation of a Location Parameter. *The Annals of Mathematical Statistics* 35, 1 (1964), 73–101.

[24] Lee Hyunwook and Ko Sungahn. 2024. TESTAM: A Time-Enhanced Spatio-Temporal Attention Model with Mixture of Experts. In *The Twelfth International Conference on Learning Representations*.

[25] Jiahao Ji, Jingyuan Wang, Chao Huang, Junjie Wu, Boren Xu, Zhenhe Wu, Junbo Zhang, and Yu Zheng. 2023. Spatio-temporal self-supervised learning for traffic flow prediction. In *Proceedings of the AAAI Conference on Artificial Intelligence*,

- Vol. 37. 4356–4364.
- [26] Xu Jia, Bert De Brabandere, Tinne Tuytelaars, and Luc V Gool. 2016. Dynamic filter networks. *Advances in neural information processing systems* 29 (2016).
  - [27] Jiawei Jiang, Chengkai Han, Wayne Xin Zhao, and Jingyuan Wang. 2023. PDFFormer: Propagation Delay-aware Dynamic Long-range Transformer for Traffic Flow Prediction. In *AAAI AAAI Press*.
  - [28] Renhe Jiang, Zhaonan Wang, Yudong Tao, Chuang Yang, Xuan Song, Ryosuke Shibasaki, Shu-Ching Chen, and Mei-Ling Shyu. 2023. Learning Social Meta-knowledge for Nowcasting Human Mobility in Disaster. In *Proceedings of the ACM Web Conference 2023*. 2655–2665.
  - [29] Renhe Jiang, Zhaonan Wang, Jiawei Yong, Puneet Jeph, Quanjun Chen, Yasumasa Kobayashi, Xuan Song, Shintaro Fukushima, and Toyotaro Suzumura. 2023. Spatio-temporal meta-graph learning for traffic forecasting. In *Proceedings of the AAAI Conference on Artificial Intelligence*, Vol. 37. 8078–8086.
  - [30] Renhe Jiang, Du Yin, Zhaonan Wang, Yizhuo Wang, Jiewen Deng, Hangchen Liu, Zekun Cai, Jinliang Deng, Xuan Song, and Ryosuke Shibasaki. 2021. DL-traffic: Survey and benchmark of deep learning models for urban traffic prediction. In *Proceedings of the 30th ACM international conference on information & knowledge management*. 4515–4525.
  - [31] Ming Jin, Huan Yee Koh, Qingsong Wen, Daniele Zambon, Cesare Alippi, Geoffrey I Webb, Irwin King, and Shirui Pan. 2023. A survey on graph neural networks for time series: Forecasting, classification, imputation, and anomaly detection. *arXiv preprint arXiv:2307.03759* (2023).
  - [32] Yilun Jin, Kai Chen, and Qiang Yang. 2023. Transferable Graph Structure Learning for Graph-based Traffic Forecasting Across Cities. In *Proceedings of the 29th ACM SIGKDD Conference on Knowledge Discovery and Data Mining*. 1032–1043.
  - [33] Guokun Lai, Wei-Cheng Chang, Yiming Yang, and Hanxiao Liu. 2018. Modeling long-and short-term temporal patterns with deep neural networks. In *The 41st international ACM SIGIR conference on research & development in information retrieval*. 95–104.
  - [34] Shiyong Lan, Yitong Ma, Weikang Huang, Wenwu Wang, Hongyu Yang, and Pyang Li. 2022. Dstagn: Dynamic spatial-temporal aware graph neural network for traffic flow forecasting. In *International conference on machine learning*. PMLR, 11906–11917.
  - [35] Hyunwook Lee, Seungmin Jin, Hyeshin Chu, Hongkyu Lim, and Sungahn Ko. 2022. Learning to Remember Patterns: Pattern Matching Memory Networks for Traffic Forecasting. In *International Conference on Learning Representations*.
  - [36] Mengzhang Li and Zhanxing Zhu. 2021. Spatial-Temporal Fusion Graph Neural Networks for Traffic Flow Forecasting. In *Proceedings of the AAAI Conference on Artificial Intelligence*, Vol. 35. 4189–4196.
  - [37] Yaguang Li, Rose Yu, Cyrus Shahabi, and Yan Liu. 2018. Diffusion Convolutional Recurrent Neural Network: Data-Driven Traffic Forecasting. In *International Conference on Learning Representations*.
  - [38] Fan Liu, Weijia Zhang, and Hao Liu. 2023. Robust Spatiotemporal Traffic Forecasting with Reinforced Dynamic Adversarial Training. In *Proceedings of the 29th ACM SIGKDD Conference on Knowledge Discovery and Data Mining*.
  - [39] Hangchen Liu, Zheng Dong, Renhe Jiang, Jiewen Deng, Jinliang Deng, Quanjun Chen, and Xuan Song. 2023. Spatio-temporal adaptive embedding makes vanilla transformer sota for traffic forecasting. In *Proceedings of the 32nd ACM International Conference on Information and Knowledge Management*. 4125–4129.
  - [40] Xu Liu, Yutong Xia, Yuxuan Liang, Junfeng Hu, Yiwei Wang, Lei Bai, Chao Huang, Zhenguang Liu, Bryan Hooi, and Roger Zimmermann. 2023. LargeST: A Benchmark Dataset for Large-Scale Traffic Forecasting. *arXiv preprint arXiv:2306.08259* (2023).
  - [41] Yong Liu, Tengge Hu, Haoran Zhang, Haixu Wu, Shiyu Wang, Lintao Ma, and Mingsheng Long. 2023. iTransformer: Inverted Transformers Are Effective for Time Series Forecasting. *arXiv preprint arXiv:2310.06625* (2023).
  - [42] Bin Lu, Xiaoying Gan, Weinan Zhang, Huaxiu Yao, Luoyi Fu, and Xinbing Wang. 2022. Spatio-Temporal Graph Few-Shot Learning with Cross-City Knowledge Transfer. In *Proceedings of the 28th ACM SIGKDD Conference on Knowledge Discovery and Data Mining*. 1162–1172.
  - [43] Zhongjian Lv, Jiajie Xu, Kai Zheng, Hongzhi Yin, Pengpeng Zhao, and Xiaofang Zhou. 2018. Lc-rnn: A deep learning model for traffic speed prediction.. In *IJCAI*, Vol. 2018. 27th.
  - [44] Xiaolei Ma, Zhimin Tao, Yinhai Wang, Haiyang Yu, and Yunpeng Wang. 2015. Long short-term memory neural network for traffic speed prediction using remote microwave sensor data. *Transportation Research Part C: Emerging Technologies* 54 (2015).
  - [45] Aaron van den Oord, Sander Dieleman, Heiga Zen, Karen Simonyan, Oriol Vinyals, Alex Graves, Nal Kalchbrenner, Andrew Senior, and Koray Kavukcuoglu. 2016. Wavenet: A generative model for raw audio. *arXiv preprint arXiv:1609.03499* (2016).
  - [46] Bei Pan, Ugur Demiryurek, and Cyrus Shahabi. 2012. Utilizing real-world transportation data for accurate traffic prediction. In *2012 IEEE 12th international conference on data mining*. IEEE, 595–604.
  - [47] Zheyi Pan, Yuxuan Liang, Weifeng Wang, Yong Yu, Yu Zheng, and Junbo Zhang. 2019. Urban traffic prediction from spatio-temporal data using deep meta learning. In *Proceedings of the 25th ACM SIGKDD International Conference on Knowledge Discovery & Data Mining*. 1720–1730.
  - [48] Zheyi Pan, Wentao Zhang, Yuxuan Liang, Weinan Zhang, Yong Yu, Junbo Zhang, and Yu Zheng. 2020. Spatio-temporal meta learning for urban traffic prediction. *IEEE Transactions on Knowledge and Data Engineering* 34, 3 (2020), 1462–1476.
  - [49] Jürgen Schmidhuber. 1992. Learning to control fast-weight memories: An alternative to dynamic recurrent networks. *Neural Computation* 4, 1 (1992), 131–139.
  - [50] Chao Shang, Jie Chen, and Jinbo Bi. 2021. Discrete Graph Structure Learning for Forecasting Multiple Time Series. In *International Conference on Learning Representations*.
  - [51] Zezhi Shao, Fei Wang, Yongjun Xu, Wei Wei, Chengqing Yu, Zhao Zhang, Di Yao, Guangyin Jin, Xin Cao, Gao Cong, et al. 2023. Exploring Progress in Multivariate Time Series Forecasting: Comprehensive Benchmarking and Heterogeneity Analysis. *arXiv preprint arXiv:2310.06119* (2023).
  - [52] Zezhi Shao, Zhao Zhang, Fei Wang, Wei Wei, and Yongjun Xu. 2022. Spatial-temporal identity: A simple yet effective baseline for multivariate time series forecasting. In *Proceedings of the 31st ACM International Conference on Information & Knowledge Management*. 4454–4458.
  - [53] Chao Song, Youfang Lin, Shengnan Guo, and Huaiyu Wan. 2020. Spatial-temporal synchronous graph convolutional networks: A new framework for spatial-temporal network data forecasting. In *Proceedings of the AAAI conference on artificial intelligence*, Vol. 34. 914–921.
  - [54] James H Stock and Mark W Watson. 2001. Vector autoregressions. *Journal of Economic perspectives* 15, 4 (2001), 101–115.
  - [55] Laurens Van der Maaten and Geoffrey Hinton. 2008. Visualizing data using t-SNE. *Journal of machine learning research* 9, 11 (2008).
  - [56] Lelitha Vanajakshi and Laurence R Rilett. 2004. A comparison of the performance of artificial neural networks and support vector machines for the prediction of traffic speed. In *IEEE Intelligent Vehicles Symposium, 2004*. IEEE, 194–199.
  - [57] Ashish Vaswani, Noam Shazeer, Niki Parmar, Jakob Uszkoreit, Llion Jones, Aidan N Gomez, Łukasz Kaiser, and Illia Polosukhin. 2017. Attention is all you need. *Advances in neural information processing systems* 30 (2017).
  - [58] Qingsong Wen, Tian Zhou, Chaoli Zhang, Weiqi Chen, Ziqing Ma, Junchi Yan, and Liang Sun. 2023. Transformers in time series: A survey. In *International Joint Conference on Artificial Intelligence (IJCAI)*.
  - [59] Haixu Wu, Jiehui Xu, Jianmin Wang, and Mingsheng Long. 2021. Autoformer: Decomposition transformers with auto-correlation for long-term series forecasting. *Advances in Neural Information Processing Systems* 34 (2021), 22419–22430.
  - [60] Zonghan Wu, Shirui Pan, Guodong Long, Jing Jiang, Xiaoju Chang, and Chengqi Zhang. 2020. Connecting the dots: Multivariate time series forecasting with graph neural networks. In *Proceedings of the 26th ACM SIGKDD international conference on knowledge discovery & data mining*. 753–763.
  - [61] Zonghan Wu, Shirui Pan, Guodong Long, Jing Jiang, and Chengqi Zhang. 2019. Graph wavenet for deep spatial-temporal graph modeling. In *Proceedings of the 28th International Joint Conference on Artificial Intelligence*. 1907–1913.
  - [62] Yutong Xia, Yuxuan Liang, Haomin Wen, Xu Liu, Kun Wang, Zhengyang Zhou, and Roger Zimmermann. 2023. Deciphering Spatio-Temporal Graph Forecasting: A Causal Lens and Treatment. In *Thirty-seventh Conference on Neural Information Processing Systems*.
  - [63] Congxi Xiao, Jingbo Zhou, Jizhou Huang, Tong Xu, and Hui Xiong. 2023. Spatial Heterophily Aware Graph Neural Networks. *arXiv preprint arXiv:2306.12139* (2023).
  - [64] Junchen Ye, Leilei Sun, Bowen Du, Yanjie Fu, and Hui Xiong. 2021. Coupled Layer-wise Graph Convolution for Transportation Demand Prediction. In *Proceedings of the AAAI Conference on Artificial Intelligence*, Vol. 35. 4617–4625.
  - [65] Bing Yu, Haoteng Yin, and Zhanxing Zhu. 2018. Spatio-temporal graph convolutional networks: a deep learning framework for traffic forecasting. In *Proceedings of the 27th International Joint Conference on Artificial Intelligence*. 3634–3640.
  - [66] Yuan Yuan, Jingtao Ding, Chenyang Shao, Depeng Jin, and Yong Li. 2023. Spatio-temporal Diffusion Point Processes. In *Proceedings of the 29th ACM SIGKDD Conference on Knowledge Discovery and Data Mining*.
  - [67] Chuanpan Zheng, Xiaoliang Fan, Cheng Wang, and Jianzhong Qi. 2020. Gman: A graph multi-attention network for traffic prediction. In *Proceedings of the AAAI conference on artificial intelligence*, Vol. 34. 1234–1241.
  - [68] Haoyi Zhou, Shanghang Zhang, Jieqi Peng, Shuai Zhang, Jianxin Li, Hui Xiong, and Wancai Zhang. 2021. Informer: Beyond efficient transformer for long sequence time-series forecasting. In *Proceedings of the AAAI conference on artificial intelligence*, Vol. 35. 11106–11115.
  - [69] Tian Zhou, Ziqing Ma, Qingsong Wen, Xue Wang, Liang Sun, and Rong Jin. 2022. Fedformer: Frequency enhanced decomposed transformer for long-term series forecasting. In *International Conference on Machine Learning*. PMLR, 27268–27286.
  - [70] Zhengyang Zhou, Qihe Huang, Gengyu Lin, Kuo Yang, Lei Bai, and Yang Wang. 2022. Greto: remedying dynamic graph topology-task discordance via target homophily. In *The eleventh international conference on learning representations*.
  - [71] Zhengyang Zhou, Kuo Yang, Yuxuan Liang, Binwu Wang, Hongyang Chen, and Yang Wang. 2023. Predicting collective human mobility via countering spatiotemporal heterogeneity. *IEEE Transactions on Mobile Computing* (2023).

## A APPENDIX

### A.1 Notation Table

For reference, Table 6 summarizes the key notations and their descriptions in this paper.

**Table 6: Notations and their descriptions.**

Notation	Description
$B$	Batch size.
$N$	Number of spatial locations.
$T, \mathcal{T}$	Number of time steps.
$X, X^b / \hat{X}$	Input/output time series.
$E_t, E_s, E_{st}$	Embedding matrices.
$d_{tod}, d_{dow}, d_t, d_s, d_{st}$	Embedding dimensions.
$\Theta, \Theta', \Theta_t, \Theta_s, \Theta_{st}$	Parameter spaces.
$P, P_t, P_s, P_{st}$	Meta-parameter pools.
$\vartheta, \vartheta_t, \vartheta_s, \vartheta_{st}$	Meta-parameters.
$S$	Parameter size.
$H, h$	GCRU hidden encoding and its size.
$\hat{A}, \hat{A}_{st}$	Adaptive graph adjacency matrices.

### A.2 Training Settings

For reproducibility, we provide details of our training settings in Table 7. Different values used for METRLA, PEMS04, PEMS07, and PEMS08 are separated by slashes.

**Table 7: Detailed training settings.**

Configuration	METRLA/PEMS04/PEMS07/PEMS08
Batch size ( $B$ )	16
Optimizer	Adam
Weight decay	0.0005/0.0001/0.0001/0.0001/0
Epsilon	0.001
Learning rate (LR)	0.001
Scheduler milestones	[30, 40]/[25, 35]/[30, 50]/[40, 60]/[40, 60, 80]
Scheduler LR decay	0.1
Early stop patience	20
Max number of epochs	200
Gradient clip	5

### A.3 Efficiency Report

All the experiments are performed on an Intel(R) Xeon(R) Silver 4310 CPU @ 2.10GHz, 256G RAM computing server, equipped with NVIDIA GeForce RTX 3090 graphics cards. We report the total training time and memory cost in Figure 7. Even for the largest dataset PEMS07 (883 sensors), our memory usage is still under 24GB, allowing running all benchmarks on a single RTX 3090 GPU.

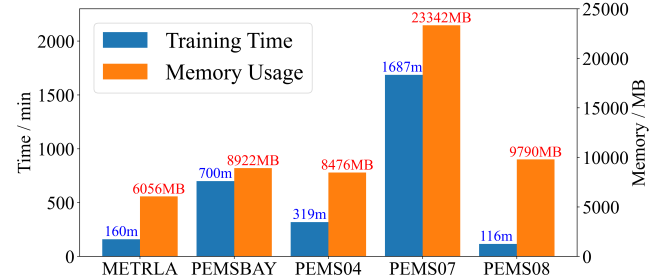


**Figure 7: Summary of training time and memory cost.**